Biochemistry and Biophysics Reports 7 (2016) 70–76

Contents lists available at ScienceDirect

Biochemistry and Biophysics Reports

journal homepage: www.elsevier.com/locate/bbrep

RP S19 C-terminal peptide trimer acts as a C5a receptor antagonist

Hiroshi Nishiura [a,*], Toru Kawakami [b], Mutsuki Kawabe [a], Nahoko Kato-Kogoe [a], Naoko Yamada [a], Keiji Nakasho [a], Koji Yamanegi [a]

[a] Department of Pathology, Hyogo College of Medicine, 1-1 Mukogawa-cho, Nishinomiya, Hyogo 663-8501, Japan
[b] Institute for Protein Research, Osaka University, 3-2 Yamadaoka, Suita, Osaka 565-0871, Japan

ARTICLE INFO

Article history:
Received 28 February 2016
Received in revised form
30 April 2016
Accepted 9 May 2016
Available online 10 May 2016

Keywords:
Antagonist
C5a receptor
Neutrophils
P38 MAPK
Ribosomal protein S19
Trimer

ABSTRACT

We have demonstrated that ribosomal protein S19 (RP S19) polymer, when crosslinked between Lys122 and Gln137 by activated coagulation factor XIII, acts as a C5a receptor (C5aR) antagonist/agonist. Based on experimental data obtained using RP S19 analog peptide and recombinant protein monomer, we suggested that L_{131}DR, I_{134}AGQVAAAN and K_{143}KH moieties in the RP S19 C-terminus act in, respectively, C5aR binding, penetration of the plasma membrane, and interaction with either an apoptosis-inducing molecule in neutrophils (delta lactoferrin) or a calcium channel-activating molecule (annexin A3) to induce the p38 MAPK pathway in macrophages. Recently, we observed RP S19 trimer in serum. To study the effects of this RP S19 trimer on C5aR, we prepared mutant RP S19 C-terminal peptide (RP $S19^{122\text{-}145}$) dimer and trimer, and examined their chemotactic activities and signal transduction pathways in human C5aR-overexpressing squamous cell carcinoma HSC-1 (HSC-1^{C5aR}) cells using 24 trans-well chamber and western blotting assays, respectively. HSC-1^{C5aR} cells were attracted by RP $S19^{122\text{-}145}$ dimer and vice versa by RP $S19^{122\text{-}145}$ trimer. The RP $S19^{122\text{-}145}$ dimer-induced attraction was competitively blocked by pre-treatment with RP $S19^{122\text{-}145}$ trimer. Moreover, RP $S19^{122\text{-}145}$ trimer-induced p38 MAPK phosphorylation was stronger than RP $S19^{122\text{-}145}$ dimer-induced p38 MAPK phosphorylation. RP $S19^{122\text{-}145}$ trimer appeared to act as a C5aR antagonist. The agonistic and antagonistic effects of RP $S19^{122\text{-}145}$ dimers and trimers were reflected by monocytic, THP-1-derived macrophage-like cells. Unlike the C5aR agonist C5a, which acts at the inflammation phase of acute inflammation, RP S19 trimer might act as a C5aR antagonist at the resolution phase.

1. Introduction

C5a is generally cleaved from C5 (a plasma protein released from hepatocytes) by C5 convertase at the inflammatory phase of acute inflammation [1]. The chemotactic potency of neutrophils is usually suppressed in C5-deficient acute inflammation mouse models [2]. Therefore, we believe that C5a functions as a neutrophil C5a receptor (C5aR) agonist to transmit a pro-inflammatory signal. Based on the NMR structure of C5a and experiments in which C5aR is mutated, the C5a C-terminus (L_{72}GR) has been suggested to bind to C5aR-activating sites [3,4]. When the GDP form of the Gαi2 subunit is exchanged with the GTP form of this subunit via the guanidine exchange factor activity of C5aR, the Gβγ subunits commonly interact with phospholipase Cβ2 in an intracellular calcium-dependent manner. After intracellular calcium is released, the calcium channel on the plasma membrane is activated (opened), thereby inducing cell motility through the signals of phosphatidylinositol 3-kinase and the extracellular signal-regulated protein kinases 1/2 (ERK1/2). The C5aR C-terminal phosphorylation that is downstream of the ERK1/2 pathway induces receptor internalization to restrict excessive neutrophil action. The C5aR gene is known not to have splice variant mRNAs [5]. However, excessive neutrophil activation is sometimes observed during the resolution phase in C5aR-deficient acute inflammation mouse models [6,7].

We purified S19 ribosomal protein (RP S19) polymer as a monocyte-specific chemoattractant in rheumatoid arthritis synovial tissue extracts [8]. In this case, RP S19 monomers in apoptotic cells are crosslinked between Lys122 and Gln137 due to the activation of tissue transglutaminases. Conversely, RP S19 monomers in plasma move to phosphatidylserine on platelets during acute inflammation and are crosslinked due to the activation of coagulation factor XIII [9]. Based on data obtained using mutated

Abbreviations: ANXA3, annexin A3; C5aR, C5a receptor; HSC-1^{C5aR}, C5aR-overexpressing human squamous cell carcinoma HSC-1; δLf, delta lactoferrin; ERK1/2, extracellular signal-regulated protein kinases 1/2; RP $S19^{122\text{-}145}$, mutant RP $S19^{122\text{-}145}$ peptide; p38 MAPK, p38 mitogen-activated protein kinase; RP S19, S19 ribosomal protein

* Corresponding author.
E-mail addresses: hi-nishiura@hyo-med.ac.jp (H. Nishiura), kawa@protein.osaka-u.ac.jp (T. Kawakami), muttsu@hyo-med.ac.jp (M. Kawabe), nkogoe@hyo-med.ac.jp (N. Kato-Kogoe), ynaoko@hyo-med.ac.jp (N. Yamada), keita@hyo-med.ac.jp (K. Nakasho), yamanegi@hyo-med.ac.jp (K. Yamanegi).

http://dx.doi.org/10.1016/j.bbrep.2016.05.006

crosslinked RP S19 recombinant protein, the RP S19 dimer attracted monocytes/macrophages but not neutrophils [10]. Moreover, L_{131}DR and I_{134}AGQVAAANKKH moieties located in the RP S19 C-terminus functioned in C5aR binding and in antagonistic or agonistic switching, respectively. To examine the cell type-specific switching mechanism, we prepared the Gly73Asn mutant of C5a recombinant protein containing I_{134}AGQVAAANKKH, C5a/RP S19. Interestingly, partner molecules to C5a/RP S19 include delta lactoferrin (δLf) in neutrophils and full-length annexin A3 (ANXA3) in macrophages [11,12]. δLf is a transcription factor that induces apoptosis. Conversely, ANXA3 is an activator that opens calcium channels on the plasma membrane to transmit signals in the p38 mitogen-activated protein kinase (p38 MAPK) pathway. Therefore, we suggested that the RP S19 polymer functions as a cell-specific C5aR antagonist/agonist.

The RP S19 monomer in plasma and the corresponding polymer in serum were detected using anti-RP S19 rabbit IgGs [13]. Especially, RP S19 polymer was cross-reacted with anti-C5a rabbit IgGs. We recently observed a band at 50 kDa that reacted with both anti-RP S19 and anti-C5a rabbit IgGs using western blotting, as previously shown in guinea pig serum [14,15]. To study the roles of the RP S19 trimer in serum, we newly prepared the mutant RP $S19^{122\text{-}145}$ peptide (RP $S19^{122\text{-}145}$) trimer and C5aR-overexpressing human squamous cell carcinoma HSC-1 (HSC-1^{C5aR}) cells. The RP $S19^{122\text{-}145}$ trimer appeared to work as a C5aR antagonist through inducing a strong p38 MAPK signal. The RP S19 trimer most likely acts as a C5aR antagonist during the resolution phase of acute inflammation.

2. Materials and methods

2.1. Reagents

The RP S19 C-terminus (K_{122}LTPQGQRDLDRIAGQVAAANKKH) peptide (the RP $S19^{122\text{-}145}$ monomer) was prepared using Fmoc-solid phase synthesis and an automated peptide synthesizer (Liberty Blue; CEM Corporation, NC, USA); Fmoc-NH-SAL resin was used to prepare the C-terminal amide, and H-His(Trt)-Trt(2-Cl) resin was used to prepare the C-terminal acid (Watanabe Chemical Ind., Hiroshima, Japan) (Fig. 1A). The peptides were purified using reversed-phase high performance liquid chromatography (HPLC) and C18 columns (Nacalai tesque, Kyoto, Japan); the identity of the peptides was confirmed by mass spectrometry using Autoflex (Bruker Daltonics, MA, USA) or LCQDeca XP Plus (Thermo Scientific, MA, USA) instruments and quantitative amino acid analysis. The RP $S19^{122\text{-}145}$ dimer (linked by triazole) was prepared using Click chemistry (Fig. 1C) [16]. Thus, the RP $S19^{122\text{-}145}$ trimer was linked by thioether and triazole bonds (Fig. 1D).

Ac-RP $S19^{122\text{-}145\text{-}Asp\text{-}Gly\text{-}Gly\text{-}Cys\text{-}NH2}$ was fluorescence-labeled at the C-terminal Cys residue as a thioether by reaction with Alexa Fluor 568 C5 (Invitrogen, CA, USA) (RP $S19^{122\text{-}145\text{-}Cysalkyl\text{-}Cy5}$ monomer) (Fig. 2A) or as a disulfide by reaction with a reagent that was prepared by reacting Alexa Fluor 568 C5, NHS ester and 2-aminoethyl methanethiosulfonate (RP $S19^{122\text{-}145\text{-}CysSS\text{-}Cy5}$ monomer) (Fig. 2B).

2.2. Vector and HSC-1 cells

To generate HSC-1 transformed cells, pCMV6-C5aR1-GFP cDNA (NM_001736) (OriGene Technology, Inc. MD, USA) was cleaved using EcoRI restriction enzyme (TAKARA, Kyoto, Japan) and transferred into HSC-1 cells (RIKEN BioResource Center, Tukuba, Japan) using a NAPA21 electroplater (Nepa Gene Co., Ltd. Chiba, Japan) according to a protocol that was approved by the Research Ethics Committee of the Japanese Hyogo College of Medicine (No. 1793) in accordance with the Helsinki Declaration of 1975, as revised in 2002. Successfully transformed cells (HSC-1^{C5aR} cells) were sorted using a BD FACSAria™III Cell Sorter (BD bioscience, Tokyo, Japan). The optimal clone was selected based on growth rate and sensitivity to the RP $S19^{122\text{-}145}$ monomer. Morphological

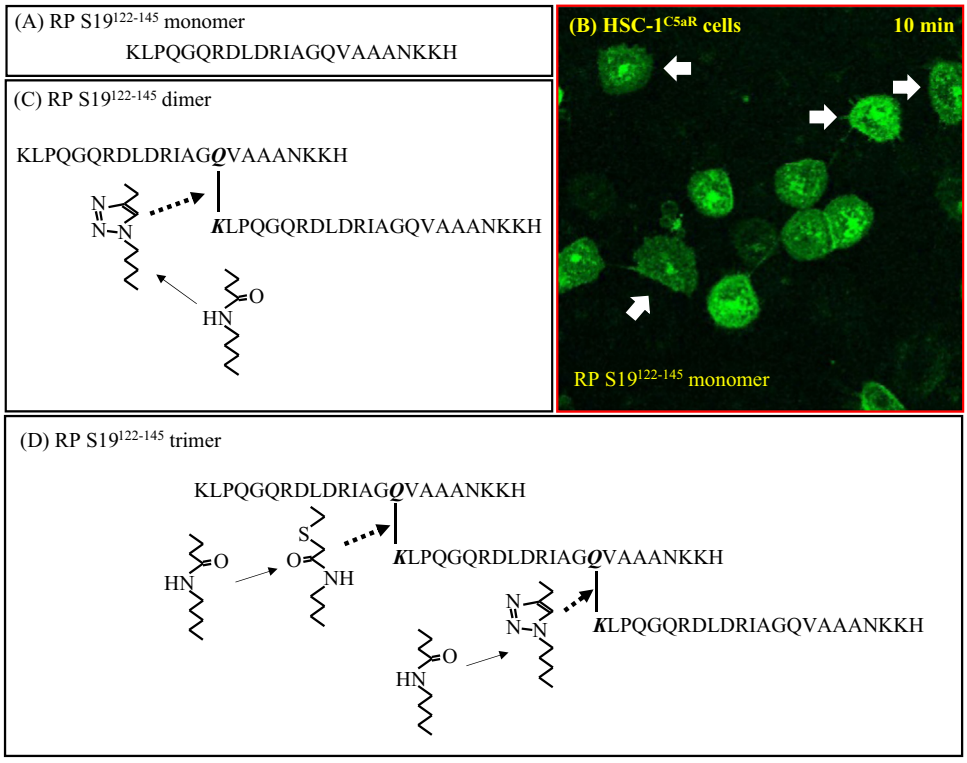

Fig. 1. Activation of HSC-1^{C5aR} cells by the RP $S19^{122\text{-}145}$ monomer. (A, C, D) Schematic models of the RP $S19^{122\text{-}145}$ monomer, dimer and trimer, in which the isopeptide skeleton is replaced with a triazole or thioether skeleton for synthetic reasons. (B) A representative morphological change of HSC-1^{C5aR} cells is shown (white arrow); the image was obtained using fluorescence microscopy 10 min after the stimulation (× 100) (n=6).

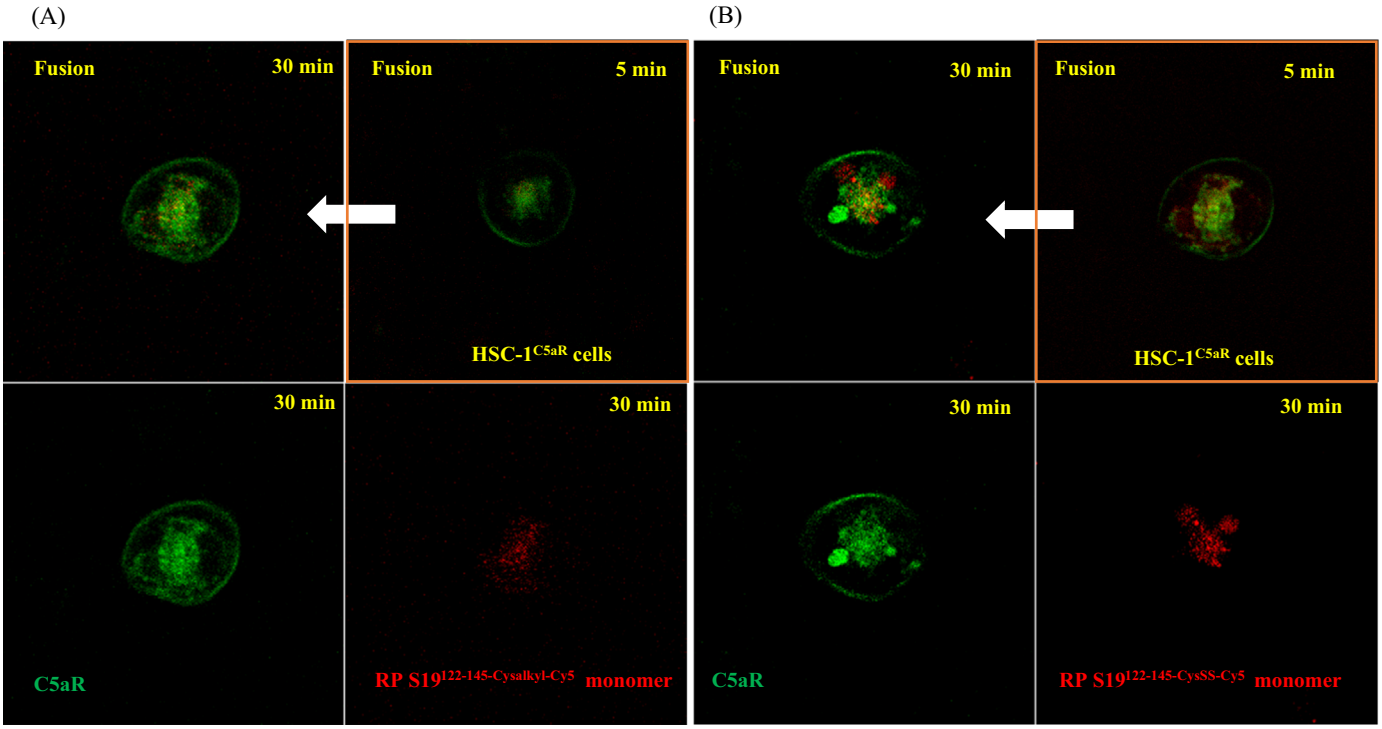

Fig. 2. Localization of the RP S19$^{122\text{-}145}$ monomer C-terminus in HSC-1^{C5aR} cells. The positions of the RP S19$^{122\text{-}145\text{-}Cysalkyl\text{-}Cy5}$ monomer (A) and the RP S19$^{122\text{-}145\text{-}CysSS\text{-}Cy5}$ monomer (B) were observed by laser scanning microscopy in HSC-1^{C5aR} cells at 5 min and 30 min after the stimulation (n=6). Representative positions of C5aR and the peptide C-terminus are shown as green or red dots in the lower left or right 30-min images. Yellow dots in the fused images are only shown in the upper right 30 min image.

changes of HSC-1^{C5aR} cells were usually observed using a Ti-E immunofluorescence microscope (Nikon, Tokyo, Japan). For analyses of Cy5 localization, HSC-1^{C5aR} cells were observed using an Axiovert/LSM510 instrument (Carl Zeiss, North Ryde, Australia).

2.3. Chemotaxis assay

HSC-1^{C5aR} cells (4×10^5 cells/mL) were prepared in DMEM medium containing 10% FBS and 100 U penicillin/streptomycin for a chemotaxis assay in a 24-well trans-well chamber [17]. 1×10^5 indicator cells in 250 μL and 10^{-6} M chemoattractants in 1 mL of the same cell culture medium were applied to the upper chamber equipped with an 8-μm pore filter and the lower chamber, respectively.

First, 1×10^5 monocytic THP-1 cells (RIKEN BioResource Center, Tsukuba, Japan) in 250 μL of the cell culture medium containing 100 nM phorbol 12-myristate 13-acetate (PMA) (the cell differentiation medium) and 1 mL of the same differentiation medium were applied to the upper and lower chambers, respectively. After one day, the cell differentiation medium in the lower or upper chambers was changed to the cell culture medium with or without 10^{-6} M of chemoattractants.

After 6 h of culture in an incubator under 5% CO_2 at 37 °C with 85% humidity, the number of cells that migrated from the upper chamber to the lower chamber was counted using the trypan-blue dye exclusion method; at least 3 wells were counted in each of 4 different experiments.

2.4. Sodium dodecyl sulfate polyacrylamide gel electrophoresis and Western blotting

Total proteins of HSC-1^{C5aR} cells were suspended in lysis buffer (7 M urea, 2 M thiourea, 1% Triton X-100, 18 mM dithiothreitol, and 0.1% bromothymol blue) and applied to 12% SDS-polyacrylamide gel electrophoresis gels. The proteins were electrophoretically transferred to an Immobilon Transfer Membrane™ (Millipore, MA, USA) using a semi-dry electroblotter (Sartorius, Göttingen, BRD) for 90 min using a current of 15 V. Phosphorylated and nonphosphorylated anti-p38 MAPK or anti-ERK1/2 rabbit IgGs were obtained from Cell Signaling Technology (MA, USA). Primary antibodies (200 ng/mL) were incubated for 1 h at 22 °C, and HRP-conjugated anti-rabbit IgGs goat IgGs secondary antibody (20 ng/mL; Santa Cruz Biotechnology, CA, USA) was incubated for 30 min at 22 °C. The signals were detected using the ECL-Plus Western Blotting Detection System™ (GE Healthcare, Tokyo, Japan). The phosphorylation ratio of p38 MAPK to ERK1/2 was calculated based on the non-phosphorylated band densities in Western blots using ImageJ 1.46 (National Institutes of Health, MD, USA).

2.5. Statistical analysis

Each result was confirmed in multiple experiments using a minimum of three samples. Statistical significance was calculated by non-parametric and parametric tests with two-way analysis of variance. The values are presented as the means ± SD. A P-value < 0.05 was considered statistically significant, and the results are presented as $P < 0.05$ (*) or $P < 0.01$ (**).

3. Results and discussion

3.1. The roles of the RP S19 C-terminus in C5aR

RP S19 recombinant protein monomers were crosslinked due to the activation of coagulation factor XIII, and at least 4 kinds of fractions were collected by HPLC using a C4 column. The main components in fractions 1–4 were identified using sodium dodecyl sulfate polyacrylamide gel electrophoresis as the intra-crosslinked monomer and the inter-crosslinked dimer, tetramer and hexamer, respectively [18]. The purity of each fraction was at least 50%. The chemotactic activity against monocytes/macrophages was slightly

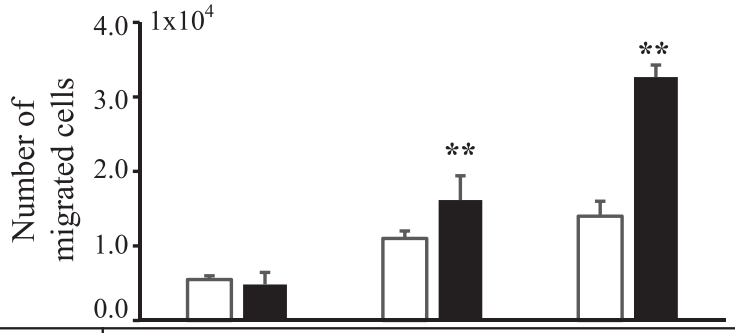

Upper chamber	cell number	10^5 cells					
	cell types	HSC-1 cells	HSC-1^{C5aR} cells	HSC-1 cells	HSC-1^{C5aR} cells	HSC-1 cells	HSC-1^{C5aR} cells
Lower chamber	concentrations	-		10^{-6} M		10^{-6} M	
	chemoattractants	Vehicle buffer		RP S19$^{122\text{-}145\text{-}Cysalkyl\text{-}Cy5}$ monomer		RP S19$^{122\text{-}145\text{-}CysSS\text{-}Cy5}$ monomer	

Fig. 3. Interaction of the RP S19$^{122\text{-}145}$ monomer with C5aR in HSC-1^{C5aR} cells. HSC-1^{C5aR} cells in the upper chamber were stimulated with vehicle buffer, RP S19$^{122\text{-}145\text{-}Cysalkyl\text{-}Cy5}$ monomer or RP S19$^{122\text{-}145\text{-}CysSS\text{-}Cy5}$ monomer in a trans-well chamber assay (n=4).

increased and that against neutrophils was not observed by any fractions. Moreover, the antagonistic/agonistic dual functions of the RP S19 polymer were reflected by both C5a/RP S19 recombinant protein and analog peptide monomers. We recently showed that RP S19 C-terminus includes three regions: the C5aR binding region (L_{131}DR), the membrane-penetrating region (I_{134}AGQVAAAN), and the antagonist/agonist switching region (K_{143}KH) [19,20]. Therefore, we suggested that the RP S19$^{122\text{-}145}$ trimer acts as a C5aR antagonist/agonist.

3.2. LDR-mediated polarization activity of the RP S19$^{122\text{-}145}$ monomer in HSC-1^{C5aR} cells

To observe the polarization activity of the RP S19$^{122\text{-}145}$ monomer in HSC-1^{C5aR} cells, 1×10^4 cells were seeded on a Φ30 mm glass-bottomed cell culture dish (Fig. 1A). After one day, 10^{-6} M RP S19$^{122\text{-}145}$ monomer was mixed with the culture medium, and the resulting morphological change of the HSC-1^{C5aR} cells was observed. Spike-like filopodia were clearly visible after 10 min (Fig. 1B white arrows). These data suggest that the K_{143}KH moiety in the RP S19$^{122\text{-}145}$ monomer interacted with ANXA3 in HSC-1^{C5aR} cells to induce the p38 MAPK pathway.

3.3. IAGQVAAAN-mediated localization of the RP S19$^{122\text{-}145}$ monomer in HSC-1^{C5aR} cells

To confirm the membrane-penetrating activity of the RP S19$^{122\text{-}145}$ monomer, 1×10^5 HSC-1^{C5aR} cells were seeded on a Φ30 mm glass-bottomed cell culture dish. After one day, 10^{-6} M RP S19$^{122\text{-}145\text{-}Cysalkyl\text{-}Cy5}$ monomer (Fig. 2(A)) or RP S19$^{122\text{-}145\text{-}CysSS\text{-}Cy5}$ monomer (Fig. 2B) was mixed with the culture medium, and the localization of the monomer in HSC-1^{C5aR} cells was observed. At 5 min after stimulation, the RP S19$^{122\text{-}145\text{-}Cysalkyl\text{-}Cy5}$ monomer C-terminus was mainly observed on the cytoplasmic side of the plasma membrane. This localization did not change until at least 30 min after stimulation. These data reflected a lack of C5aR internalization after the stimulation with C5a/RP S19 through the p38 MAPK pathway [21]. At 5 min after stimulation, the RP S19$^{122\text{-}145\text{-}CysSS\text{-}Cy5}$ monomer C-terminus was also mainly observed at the cytoplasmic side of the plasma membrane. However, the RP S19$^{122\text{-}145\text{-}CysSS\text{-}Cy5}$ monomer C-terminus moved to the cytoplasmic side at 30 min after the stimulation. Thus, -S-Cy5 in RP S19$^{122\text{-}145\text{-}CysSS\text{-}Cy5}$ monomer was probably cleaved in the cytoplasm. We did not observe any morphological changes of the HSC-1^{C5aR} cells in this experimental setting. The C-terminal modifications most likely affected the interaction of the K_{143}KH moiety with ANXA3. These data confirmed the roles of I_{134}AGQVAAAN in membrane penetration, in addition to C5aR.

3.4. The KKH-mediated chemotactic activity of RP S19$^{122\text{-}145}$ monomer on HSC-1^{C5aR} cells

To confirm the effect of the C-terminal modification of the RP S19$^{122\text{-}145}$ monomer on the K_{143}KH-ANXA3 complex-mediated chemotactic signal, HSC-1^{C5aR} cells were stimulated with the RP S19$^{122\text{-}145\text{-}Cysalkyl\text{-}Cy5}$ monomer or the RP S19$^{122\text{-}145\text{-}CysSS\text{-}Cy5}$ monomer in a trans-well chamber (Fig. 3). At 6 h after the stimulation, HSC-1^{C5aR} cells in the upper chamber significantly migrated into the lower chamber containing the RP S19$^{122\text{-}145\text{-}Cysalkyl\text{-}Cy5}$ monomer or the RP S19$^{122\text{-}145\text{-}CysSS\text{-}Cy5}$ monomer to a greater extent than HSC-1 cells. These data indicated that the -Cysalkyl-Cy5 modification but not the -CysSS-Cy5 modification to the K_{143}KH moiety of the RP S19$^{122\text{-}145}$ monomer affected the complex with ANXA3 to induce chemotaxis through the p38 MAPK pathway.

3.5. The roles of the RP S19$^{122\text{-}145}$ trimer in C5aR

To examine the roles of the RP S19$^{122\text{-}145}$ trimer in C5aR, HSC-1 cells or HSC-1^{C5aR} cells were stimulated with the monomer, the dimer or the trimer (see Fig. 1A, C, and D) in a trans-well chamber (Fig. 4A). At 6 h after the stimulation, the number of HSC-1 cells that migrated into the chamber containing any RP S19 peptides was significantly lower than the number of HSC-1^{C5aR} cells that migrated. When using vehicle buffer, no significant difference was observed. C5aR was specifically activated by RP S19$^{122\text{-}145}$ peptides. Interestingly, the chemotactic activity of the RP S19$^{122\text{-}145}$ dimer or trimer was the highest or lowest among the RP S19$^{122\text{-}145}$ peptides. The chemotactic activity of the RP S19$^{122\text{-}145}$ trimer was significantly higher than that of vehicle buffer.

To confirm the structure of the RP S19$^{122\text{-}145}$ trimer, 1×10^5 HSC-1^{C5aR} cells were mixed with 10^{-6} M RP S19$^{122\text{-}145}$ trimer or vehicle buffer for 5 min These mixtures and 10^{-6} M RP S19$^{122\text{-}145}$ dimer or trimer were applied to the upper and lower chambers, respectively (Fig. 4B). After 6 h of incubation, the number of

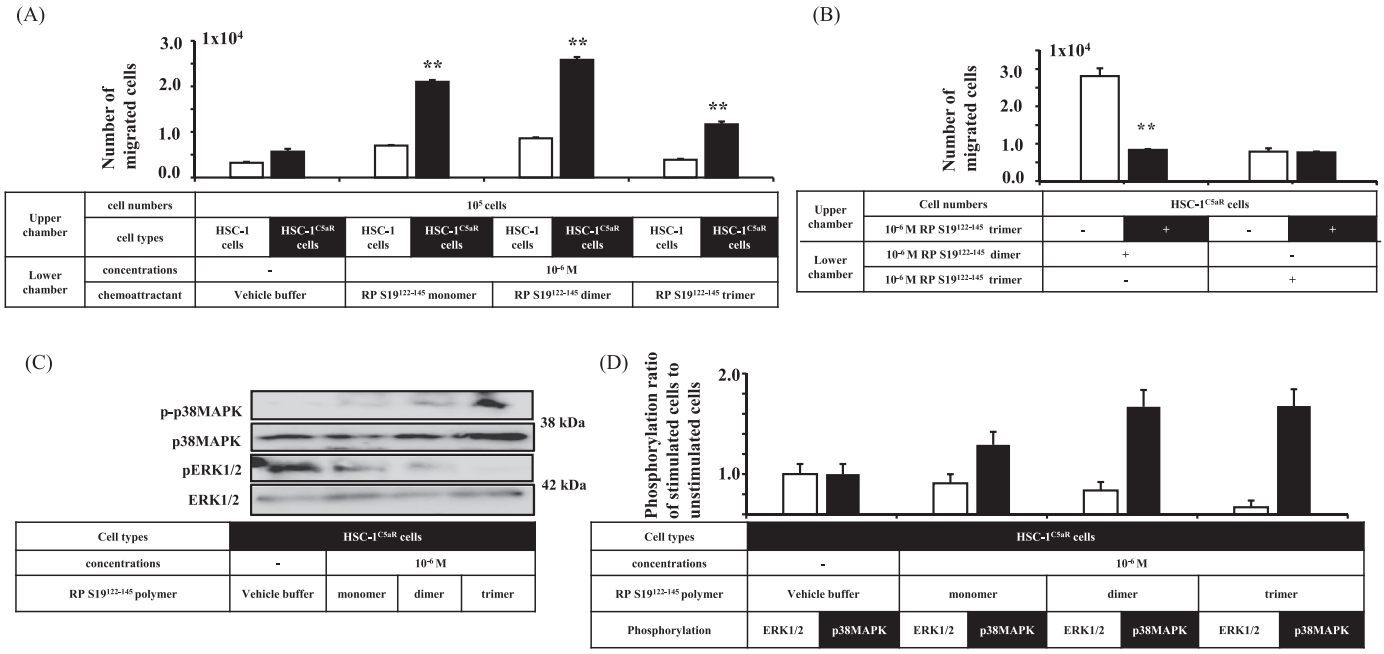

Fig. 4. RP S19$^{122-145}$ dimer and trimer acted oppositely on C5aR in HSC-1^{C5aR} cells. (A) HSC-1 cells or HSC-1^{C5aR} cells in the upper chamber were stimulated with vehicle buffer, RP S19$^{122-145}$ monomer, RP S19$^{122-145}$ dimer or RP S19$^{122-145}$ trimer in a trans-well chamber assay (n=4). (B) HSC-1^{C5aR} cells were pre-mixed with or without RP S19$^{122-145}$ trimer for 10 min, and indicator cells in the upper chamber were stimulated with RP S19$^{122-145}$ dimer or RP S19$^{122-145}$ trimer in a trans-well chamber assay (n=4). (C) HSC-1^{C5aR} cells in Φ 100 mm cell culture dish were stimulated with vehicle buffer, RP S19$^{122-145}$ monomer, RP S19$^{122-145}$ dimer or RP S19$^{122-145}$ trimer (n=4). Phosphorylated and non-phosphorylated p38MAPK and ERK1/2 proteins were detected using Western blotting. (D) The phosphorylation ratio of p38 MAPK to ERK1/2 was calculated based on the non-phosphorylated band densities in Western blots using ImageJ 1.46.

HSC-1^{C5aR} cells that migrated into the chamber containing the RP S19$^{122-145}$ dimer was significantly decreased when pre-treated with the RP S19$^{122-145}$ trimer.

To study the sensitivity of the RP S19$^{122-145}$ trimer to the C5aR-mediated p38 MAPK signal in HSC-1^{C5aR} cells, 1×10^6 cells were seeded on a Φ100 mm cell culture dish (Fig. 4C). After one day, 10^{-6} M of the monomer, dimer or trimer were mixed with culture medium for 20 min, and proteins in the attached cells were collected for Western blotting. p38 MAPK phosphorylation was highest and lowest in HSC-1^{C5aR} cells after stimulation with the RP S19$^{122-145}$ trimer and vehicle buffer. Conversely, ERK1/2 phosphorylation was highest and lowest in HSC-1^{C5aR} cells after stimulation with vehicle buffer and the RP S19$^{122-145}$ trimer. ERK1/2 phosphorylation was most likely detected via constitutively activated GPCRs. The p38 MAPK/ERK1/2 phosphorylation ratio appeared to change from antagonist to agonist (Fig. 4D). The RP S19$^{122-145}$ trimer commonly acts as a C5aR antagonist via a strong p38 MAPK signal in HSC-1^{C5aR} cells.

To explain the high p38 MAPK/ERK1/2 phosphorylation ratio in HSC^{C5aR} cells in response to RP S19$^{122-145}$ trimer in our experimental setting, we suggest that the following sequence of events occurs after the RP S19$^{122-145}$ trimer interacts with one C5aR (see Graphical Abstract): (1) any L_{131}DR moieties in the three RP S19 peptides can bind to the active pocket near the top of the 5th transmembrane of C5aR. (2) One G protein transmits one ERK1/2 signal via the active form of one C5aR. (3) All I_{133}AGQVAAAN moieties in the three RP S19 peptides penetrate the plasma membrane. (4) All K_{143}KH moieties move to the cytoplasmic side of the plasma membrane. We did not examine the affinities of the K_{143}KH moiety to ANXA3 and δLf. (5) RP S19$^{122-145}$ monomer: one p38 MAPK signal is transmitted via one K_{143}KH moiety through one ANXA3. The weak chemotaxis activity is induced via one C5aR-mediated ERK1/2 signal plus one p38 MAPK signal. (6) RP S19$^{122-145}$ dimer: one p38 MAPK signal is transmitted via one K_{143}KH moiety through one ANXA3. One RGS3 increases GTPase activity of the Gα subset via another K_{143}KH moiety through one δLf, which results in the association of the Gα and Gβγ subsets. The association of G protein decreases the C5aR-mediated ERK1/2 signal. The strong chemotaxis activity is induced via one C5aR-mediated half ERK1/2 signal plus one p38 MAPK signal. (7) RP S19$^{122-145}$ trimer: two p38 MAPK signals are transmitted via two K_{143}KH moieties through two ANXA3s. The C5aR-mediated ERK1/2 signal is decreased by one RGS3. No chemotactic activity is induced via one C5aR-mediated half ERK1/2 signal plus two p38 MAPK signals. Currently, we are interested in studying several types of RP S19$^{122-145}$ trimer interactions with C5aRs on two or three cells of the same type and with C5aRs on two or three cells of different types.

Interestingly, several reports indicate that the migration of glioma cells in response to lysophosphatidic acid is partially inhibited by the activation of the p38 MAPK pathway in response to the down-regulation of cdc-42 [22]. Conversely, the p38 MAPK-enhanced invasion of colon cancer Caco-2 and HT29cells is inhibited in response to the down-regulation of MMP-9 [23]. Also interestingly, reports indicate that the p38 MAPK signal appears to promote apoptosis in bladder carcinoma cells or cancer stem cells, as previously shown by us in apoptotic cells, including neutrophils [24,25].

3.6. The roles of the GPCR agonist trimer

Based on solution NMR and x-ray crystallography data, CXC and CC chemokines are believed to work mainly during the inflammatory phase of acute inflammation as a monomer. However, N-terminal cysteines are believed to have strong dimerization potential [26]. Experimentally, dimerization is sensitive to solution conditions, such as low pH and long ionic strength. When CCL2 and CCL4 were experimentally linked by disulfide bonds, the dimer did not bind to their receptors. Conversely, the CXCL8 dimer bound to another receptor, CXCR2 [27,28]. We recommend that all chemokine researchers attempt to purify chemokine polymers in biomaterials. We strongly suggest that a crosslinked chemokine

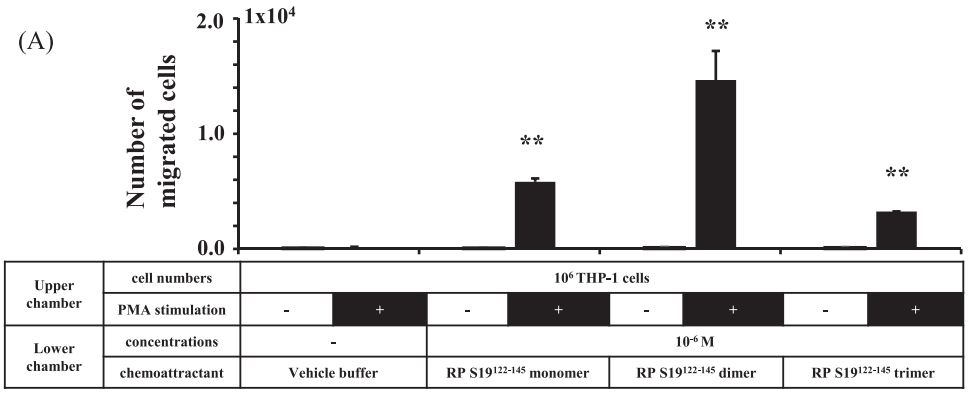

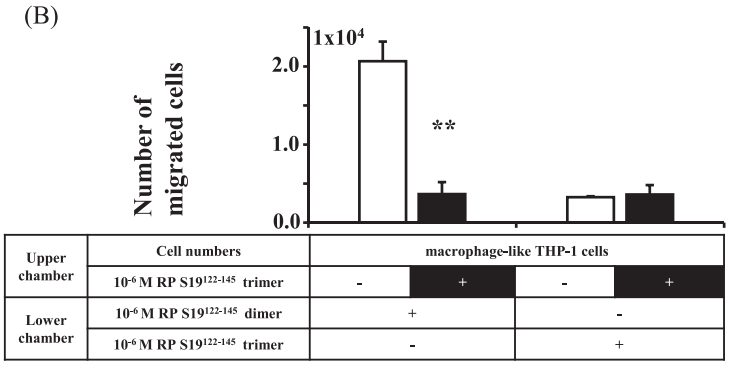

Fig. 5. RP S19$^{122-145}$ dimer and trimer acted oppositely on the C5aR in macrophage-like THP-1 cells. (A) THP-1 cells or the macrophage-like THP-1 cells in the upper chamber were stimulated with vehicle buffer, RP S19$^{122-145}$ monomer, RP S19$^{122-145}$ dimer or RP S19$^{122-145}$ trimer in a trans-well chamber assay (n=4). (B) The macrophage-like THP-1 cells were pre-mixed with or without RP S19$^{122-145}$ trimer for 10 min, and indicator cells in the upper chamber were stimulated with RP S19$^{122-145}$ dimer or RP S19$^{122-145}$ trimer in a trans-well chamber assay (n=4).

that is polymerized by factor XIIIa is present in serum.

As shown in Fig. 5, we confirmed the agonistic and antagonistic dual effects on macrophage-like THP-1 cells. THP-1 cells do not generally express δLf, which means that three p38 MAPK signals are transmitted via three K_{143}KH moieties through three ANXA3s (see Graphical Abstract). The strong p38 MAPK signals might connect directly to unknown antagonistic pathways.

Conversely, chemokine polymer research also suggests that these CXC and CC chemokines play a role in cancer metastasis. When CXCL12 monomer binds to CXCR4, Gs protein-dependent inhibition of cAMP signaling promotes metastasis [29]. In the case of the CXCL12 dimer, CXCR4 also promotes metastasis through another signal transduction pathway via the weak phosphorylation of ERK1/2. In addition, ligand-independent polymerization endows CXCR4 with an enhanced affinity for CXCL12 [30]. We need to further examine the roles of ligand-dependent polymerization.

Acknowledgments

HN and KY conceived this research; MK, NK, NY and KN developed the methodology and carried out the main experiments; TK carried out the peptide synthesis; HN analyzed the data and edited the manuscript. FACSAria™III, Ti-E and Axiovert/LSM510 were maintained in joint-use research facilities at the Hyogo College of Medicine. Grant numbers and sources of support were as follows: A Grand-in Aid for Scientific Research (C) [26462863] from the Ministry of Education, Culture, Sports, Science, and Technology. A Grand-in Aid for Researchers, Hyogo College of Medicine, 2015. This work was performed under the Cooperative Research Program of the Institute for Protein Research, Osaka University, CR-15–01.

Appendix A. Transparency Material

Transparency Material associated with this article can be found in the online version at http://dx.doi.org/10.1016/j.bbrep.2016.05.006.

References

[1] H. Nishiura, The alternative C5a receptor function, Adv. Exp. Med. Biol. 735 (2013) 111–121.
[2] G.B. Toews, W.C. Vial, The role of C5 in polymorphonuclear leukocyte recruitment in response to Streptococcus pneumoniae, Am. Rev. Respir. Dis. 129 (1984) 82–86.
[3] P.N. Monk, A.M. Scola, P. Madala, D.P. Fairlie, Function, structure and therapeutic potential of complement C5a receptors, Br. J. Pharmacol. 152 (2007) 429–448.
[4] G.V. Nikiforovich, T.J. Baranski, Structural mechanisms of constitutive activation in the C5a receptors with mutations in the extracellular loops: molecular modeling study, Proteins 80 (2012) 71–80.
[5] C. Gerard, L. Bao, O. Orozco, M. Pearson, D. Kunz, N.P. Gerard, Structural diversity in the extracellular faces of peptidergic G-protein-coupled receptors. Molecular cloning of the mouse C5a anaphylatoxin receptor, J. Immunol. 149 (1992) 2600–2606.
[6] U.E. Hopken, B. Lu, N.P. Gerard, C. Gerard, Impaired inflammatory responses in the reverse arthus reaction through genetic deletion of the C5a receptor, J. Exp. Med. 186 (1997) 749–756.
[7] G.B. Toews, A.K. Pierce, The fifth component of complement is not required for the clearance of Staphylococcus aureus, Am. Rev. Respir. Dis. 129 (1984) 597–601.
[8] H. Nishiura, Y. Shibuya, S. Matsubara, S. Tanase, T. Kambara, T. Yamamoto, Monocyte chemotactic factor in rheumatoid arthritis synovial tissue. Probably

a cross-linked derivative of S19 ribosomal protein, J. Biol. Chem. 271 (1996) 878–882.
[9] U. Semba, J. Chen, Y. Ota, N. Jia, H. Arima, H. Nishiura, T. Yamamoto, A plasma protein indistinguishable from ribosomal protein S19: conversion to a monocyte chemotactic factor by a factor XIIIa-catalyzed reaction on activated platelet membrane phosphatidylserine in association with blood coagulation, Am. J. Pathol. 176 (2010) 1542–1551.
[10] H. Nishiura, K. Tokita, Y. Li, K. Harada, T.M. Woodruff, S.M. Taylor, T.K. Nsiama, N. Nishino, T. Yamamoto, The role of the ribosomal protein S19C-terminus in Gi protein-dependent alternative activation of p38 MAP kinase via the C5a receptor in HMC-1 cells, Apoptosis 15 (2010) 966–981.
[11] H. Nishiura, K. Yamanegi, M. Kawabe, N. Kato-Kogoe, N. Yamada, K. Nakasho, Annexin A3 plays a role in cytoplasmic calcium oscillation by extracellular calcium in the human promyelocytic leukemia HL-60 cells differentiated by phorbol-12-myristate-13-acetate, Exp. Mol. Pathol. 97 (2014) 241–246.
[12] H. Nishiura, K. Yamanegi, M. Kawabe, N. Kato-Kogoe, N. Yamada, K. Nakasho, The roles of ribosomal protein S19C-terminus in a shortened neutrophil life-span through delta lactoferrin, Immunobiology (2015).
[13] H. Nishiura, J. Chen, Y. Ota, U. Semba, H. Higuchi, T. Nakashima, T. Yamamoto, Base of molecular mimicry between human ribosomal protein S19 dimer and human C5a anaphylatoxin, Int. Immunopharmacol. 10 (2010) 1541–1547.
[14] H. Nishiura, S. Tanase, K. Tsujita, S. Sugiyama, H. Ogawa, T. Nakagaki, U. Semba, T. Yamamoto, Maintenance of ribosomal protein S19 in plasma by complex formation with prothrombin, Eur. J. Haematol. 86 (2011) 436–441.
[15] M. Okamoto, T. Yamamoto, S. Matsubara, I. Kukita, M. Takeya, Y. Miyauchi, T. Kambara, Factor XIII-dependent generation of 5th Complement Component (C5)-derived Monocyte chemotactic Factor coinciding with plasma clotting, Biochim. Biophys. Acta 1138 (1992) 53–61.
[16] T.R. Chan, R. Hilgraf, K.B. Sharpless, V.V. Fokin, Polytriazoles as copper(I)-stabilizing ligands in catalysis, Org. Lett. 6 (2004) 2853–2855.
[17] H. Nomiyama, K. Hieshima, T. Nakayama, T. Sakaguchi, R. Fujisawa, S. Tanase, H. Nishiura, K. Matsuno, H. Takamori, Y. Tabira, T. Yamamoto, R. Miura, O. Yoshie, Human CC chemokine liver-expressed chemokine/CCL16 is a functional ligand for CCR1, CCR2 and CCR5, and constitutively expressed by hepatocytes, Int. Immunol. 13 (2001) 1021–1029.
[18] H. Nishiura, S. Tanase, Y. Sibuya, T. Nishimura, T. Yamamoto, Determination of the cross-linked residues in homo-dimerization of S19 ribosomal protein concomitant with exhibition of monocyte chemotactic activity, Lab. Investig. 79 (1999) 915–923.
[19] Y. Shibuya, M. Shiokawa, H. Nishiura, T. Nishimura, N. Nishino, H. Okabe, K. Takagi, T. Yamamoto, Identification of receptor-binding sites of monocyte chemotactic S19 ribosomal protein dimer, Am. J. Pathol. 159 (2001) 2293–2301.
[20] A. Shrestha, M. Shiokawa, T. Nishimura, H. Nishiura, Y. Tanaka, N. Nishino, Y. Shibuya, T. Yamamoto, Switch moiety in agonist/antagonist dual effect of S19 ribosomal protein dimer on leukocyte chemotactic C5a receptor, Am. J. Pathol. 162 (2003) 1381–1388.
[21] H. Nishiura, R. Zhao, T. Yamamoto, The role of the ribosomal protein S19C-terminus in altering the chemotaxis of leucocytes by causing functional differences in the C5a receptor response, J. Biochem. 150 (2011) 271–277.
[22] E. Malchinkhuu, K. Sato, Y. Horiuchi, C. Mogi, S. Ohwada, S. Ishiuchi, N. Saito, H. Kurose, H. Tomura, F. Okajima, Role of p38 mitogen-activated kinase and c-Jun terminal kinase in migration response to lysophosphatidic acid and sphingosine-1-phosphate in glioma cells, Oncogene 24 (2005) 6676–6688.
[23] A. Radziwon-Balicka, M.J. Santos-Martinez, J.J. Corbalan, S. O'Sullivan, A. Treumann, J.F. Gilmer, M.W. Radomski, C. Medina, Mechanisms of platelet-stimulated colon cancer invasion: role of clusterin and thrombospondin 1 in regulation of the P38MAPK-MMP-9 pathway, Carcinogenesis 35 (2014) 324–332.
[24] C.A. Neoh, R.Y. Wang, Z.H. Din, J.H. Su, Y.K. Chen, F.J. Tsai, S.H. Weng, Y.J. Wu, Induction of apoptosis by sinulariolide from soft coral through mitochondrial-related and p38MAPK pathways on human bladder carcinoma cells, Mar. Drugs 10 (2012) 2893–2911.
[25] S.P. Lin, Y.T. Lee, J.Y. Wang, S.A. Miller, S.H. Chiou, M.C. Hung, S.C. Hung, Survival of cancer stem cells under hypoxia and serum depletion via decrease in PP2A activity and activation of p38-MAPKAPK2-Hsp27, PLoS One 7 (2012) e49605.
[26] A. Ravindran, K.V. Sawant, J. Sarmiento, J. Navarro, K. Rajarathnam, Chemokine CXCL1 dimer is a potent agonist for the CXCR2 receptor, J. Biol. Chem. 288 (2013) 12244–12252.
[27] Y. Yao, S.E. Tsirka, The C terminus of mouse monocyte chemoattractant protein 1 (MCP1) mediates MCP1 dimerization while blocking its chemotactic potency, J. Biol. Chem. 285 (2010) 31509–31516.
[28] P.R. Joseph, P.D. Mosier, U.R. Desai, K. Rajarathnam, Solution NMR characterization of chemokine CXCL8/IL-8 monomer and dimer binding to glycosaminoglycans: structural plasticity mediates differential binding interactions, Biochem. J. 472 (2015) 121–133.
[29] L.J. Drury, J.J. Ziarek, S. Gravel, C.T. Veldkamp, T. Takekoshi, S.T. Hwang, N. Heveker, B.F. Volkman, M.B. Dwinell, Monomeric and dimeric CXCL12 inhibit metastasis through distinct CXCR4 interactions and signaling pathways, Proc. Natl. Acad. Sci. USA 108 (2011) 17655–17660.
[30] M. Hamatake, T. Aoki, Y. Futahashi, E. Urano, N. Yamamoto, J. Komano, Ligand-independent higher-order multimerization of CXCR4, a G-protein-coupled chemokine receptor involved in targeted metastasis, Cancer Sci. 100 (2009) 95–102.